FINITE SPOTWELD ELEMENT – HYBRID TREFFTZ FORMULATION

Thomas Heubrandtner[1], Georg Scharrer[1]

[1]The Virtual Vehicle – Competence Center (Vif),
8010 Graz, Inffeldgasse 21a, Austria

thomas.heubrandtner@v2c2.at (Thomas Heubrandtner)

Abstract

It is a well known fact that the load bearing capacity of spotwelds in car bodies has a considerable impact on the deformation behaviour under crash loads, especially on the ability of energy dissipation. Therefore it is necessary to predict spotweld failure in the crash-simulation, but there is one thing, which makes it difficult. Theoretically founded stress-/strain based failure criteria are only reasonable for a sufficiently high resolution of the local stress-/strain field of the spotweld. But unfortunately the smallest dimension of finite elements in the simulation model, limited by the conventional critical time step (explicit time integration), is far from this demand.

This paper shows a way, how the local requirements can be achieved without loss of computational performance, by the development of a finite spotweld element based on the hybrid Trefftz method. The treatment is elasto-plastic, whereas the linear elastic part as well as the rigid/perfectly-plastic part is based on a special hybrid Trefftz element representing the entire spotweld, the cylindrical nugget, heat affected zone and an annulus made of base material. These two distinct models, the linear elastic and the rigid/perfectly plastic one, are combined by a rheological approach. The linking to the residual finite element mesh, consisting of bilinear standard shells, is accomplished via a displacement frame, an arbitrary polygon. By definition the Trefftz-type solution satisfies a priori all governing differential equations within the element area and fulfils inner boundary conditions. The modeling of plastic deformation accounts for geometrically nonlinear behaviour (stress stiffening) within the metal sheet annulus and permits the forming of plastic hinges along the circumference of the comparatively rigid nugget. Isotropic hardening is considered by a piecewise perfectly-plastic cascaded flow curve, leading to a high resolution of the stress/strain field in the vicinity of the spotweld nugget, and enables the introduction of accurate stress/strain-based failure criteria; especially instability due to the onset of local necking.

Keywords: Trefftz, hybrid Trefftz, spotweld modeling, spotweld failure

Presenting Author's biography

Georg Scharrer. He finished his studies of Technical Mathematics at the University of Technology Graz in 10/2006. In 08/2005 he started doing research on a Trefftz approach for steady state acoustics at ACC Graz. Since 09/2006 he is working on enhancing a model for plastic deformation of a spotweld using a Trefftz formulation at The Virtual Vehicle Competence Center.

1 Hybrid Trefftz Formulation

Finite elements based on polynomials have proved to be an effective tool for solving partial differential equations. However, there are problems, for which good approximated solutions can only be obtained with high effort by applying standard finite elements, or it is impossible at all. These are usually problems, whose solutions or their partial derivatives can't be approximated well by polynomials used in the finite element method. That's the case for the simulation of the mechanical behaviour of a spotweld. The linear or quadratic standard shell elements are not suited for the cylinder symmetry dominating in the surrounding area of the circular spotweld nugget. The fact, that the difficulties in finding good solutions arise from these small parts of the entire structure, suggests the introduction of special finite elements, which are adapted to the local conditions via special shape functions. Suitable for this purpose proves to be a coupled pair of special Trefftz elements with a circular boundary Γ_1 within the element area Ω (Fig.1a). As per definition the shape functions satisfy the governing differential equations within Ω, and fulfil boundary conditions on inner boundary curves Γ_1. The spotweld nugget is approximately rigid compared to the adjacent sheets because the martensitic nugget has a higher yield point than the ferritic sheet, and the elastic plate bending stiffness is proportional to the 3rd power of the thickness. Thus the comparatively rigid spotweld nugget is represented by a rigid cylinder, which connects both inner circles of the Trefftz elements (Fig.1b). This linkage is implemented by coupling a pair of auxiliary nodes (Fig.1c), which lie in the center of Γ_1, and carry the spatial displacement and rotation of the spotweld nugget. In addition to the special spotweld elements, bilinear standard shells are arranged on uncritical sub-domains of the structure. The linking is accomplished via a displacement frame Γ_5, an arbitrary polygon, formed by the set of shared edges of all adjacent standard shells.
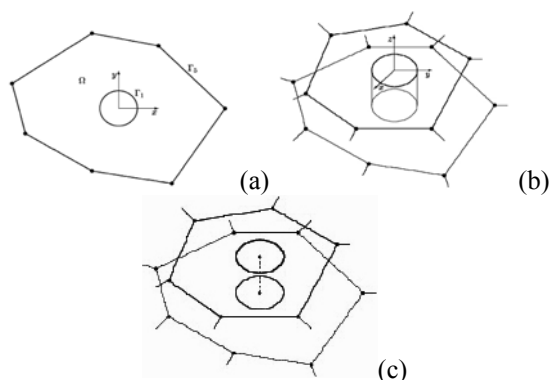

Fig. 1 (a) The Trefftz element area Ω with the circumference of the spotweld nugget Γ_1, and the polygon Γ_5 of shared edges with all adjacent standard shells. (b) Linkage of two Trefftz elements by a rigid cylinder (spotweld nugget) is accomplished via a pair of auxiliary nodes (c).

1.1 Linear Elastic Deformation

It is well known, that in the case of linear elasticity the system of thin-plate equations concerning membrane- and bending-type deformations decouple completely, so they can be dealt with separately.

1.1.1   Membrane-type deformation

Extension of the principle of minimal potential energy: The essential trick is to introduce an additional term in the potential energy leading to a weak form, which transmit the essential displacement boundary condition along the polygon into natural one. Now we have two distinct displacement fields along the polygon, which are not necessarily identical. The first comes from the solutions within the Trefftz element area, and the second one is the prescribed displacement field equal to the linked standard shells, for example, piece-wise linear between nodes. Minimization of the potential leads to a stiffness matrix which can be coupled with any other finite element with similar displacement assumptions.

The additional requirement of geometrical boundary conditions $\vec{u} = \bar{\vec{u}}$ can be avoided, if the first variation of the potential is extended by an artificial term,

$$\int_{\Gamma} \delta \vec{T}^T \left[\bar{\vec{u}} - \vec{u} \right] t\, ds , \qquad (1)$$

where t is the plate thickness and $\vec{T}$ the traction acting along the boundary Γ. Both, the displacement and stress boundary conditions are now natural conditions. The weak form (1) serves as a starting point for a technique to link Trefftz elements with adjacent bi-linear standard shells [7]. The prescribed displacement vector $\bar{\vec{u}}$ is identified with the linear boundary displacement field $\tilde{\vec{u}}$ on the closed boundary curve Γ_5,

$$\tilde{\vec{u}} = \begin{pmatrix} \tilde{\vec{U}}^T \vec{u} \\ \tilde{\vec{V}}^T \vec{v} \end{pmatrix} = \bar{\vec{u}} \qquad \text{on } \Gamma_5, \qquad (2)$$

with nodal displacements $\vec{u}$, $\vec{v}$. The vectors $\tilde{\vec{U}}$ and $\tilde{\vec{V}}$ are defined piecewise along distinct edges of the polygon Γ_5, with a total of n nodes,

$$\tilde{\vec{U}}^T(s) = \tilde{\vec{V}}^T(s) = \begin{cases} \left(1 - \dfrac{s}{s_{1,2}}, \ \dfrac{s}{s_{1,2}}, \ 0, \ 0, \ \cdots, \ 0 \right) \\ \left(0, \ 1 - \dfrac{s}{s_{2,3}}, \ \dfrac{s}{s_{2,3}}, \ 0, \ \cdots, \ 0 \right) \\ \vdots \\ \left(\dfrac{s}{s_{n,1}}, \ 0, \ 0, \ 0, \ \cdots, \ 1 - \dfrac{s}{s_{n,1}} \right) \end{cases} . \ (3)$$

The first vector refers to the edge between node 1 and 2, the second between 2 and 3, etc. Lengths of edges from node i to node j are denoted by $s_{i,j}$, and s means

the distance of an arbitrary point on an edge to its "first" corner.

1.1.2   Bending-type deformation

Bending is considered within the framework of Kirchhoff's theory of thin plates. There is an analogous extension of the first variation of the potential by an additional term

$$\int_\Gamma \delta Q [w - \overline{w}] ds + \int_\Gamma \delta \vec{M}^T [\nabla w - \nabla \overline{w}] ds \quad , \quad (4)$$

with Q and $\vec{M}$ as force acting normal to the plate, and moment twisting the boundary Γ, respectively [2]. The prescribed bending-type displacement vector, analogous $\overline{\vec{u}}$, consists of the out-of-plane displacement, $\overline{w}$, and additional rotational degrees of freedom, $\nabla \overline{w}$, with respect to axes lying within the plate-plane.

Analytic solutions: Both, membrane- and bending-type deformation can be reduced to bi-harmonic functions, Airy's stress function, $\nabla^4 U = 0$, and out-of-plane displacement, $\nabla^4 w = 0$, respectively. The general solutions are presentable by the real part $\Re[\overline{z}\Phi(z) + \Psi(z)]$ with complex potentials Φ and Ψ introduced by Kolosov-Muskhelishvili [4,5,1], and $z = x + iy$, $\overline{z} = x - iy$. An analytically deduced stress field within the Trefftz element area for an exemplary load case can be seen in Fig.2.
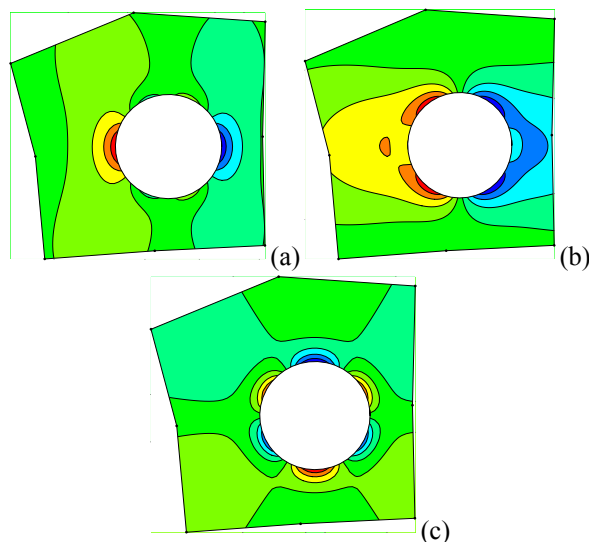

Fig. 2 Example of contour diagrams of the stress components σ_{xx} (a), σ_{yy} (b) and τ_{xy} (c) within the Trefftz element area.

1.2   Plastic Deformation – Hencky-Plasticity

We consider an rigid/perfectly-plastic isotropic material subjected to von Mises yield surface $\sigma'_{ij}\sigma'_{ij} = \frac{2}{3}Y^2$, with the deviatoric stress σ'_{ij} and tensile yield stress Y. It is additionally assumed, that

during loading the principal stress and strain ratios are held approximately constant (Hencky conditions) in the surrounding of the spotweld nugget, so the normality principle simplifies to a non-incremental form [3], $\varepsilon' = (3\overline{\varepsilon}/2\overline{\sigma})\sigma'$, with deviatoric strain ε', and equivalent strain $\overline{\varepsilon}$ and stress $\overline{\sigma}$. Within the framework of Hencky plasticity the displacement field fulfils a variational principle [6]. Anzellotti and Giaquinta showed that the perfectly plastic model can be obtained as the limit of elasto-perfectly plastic problems with yield points converging to zero. Starting from the well known variational principle (related to the displacement field $\vec{u}$) for elasto-perfectly plasticity, governed by Hencky's constitutive law, they deduce a corresponding one for rigid-perfectly plastic materials. It is given in the following form: Minimize the energy functional,

$$W_p(\vec{u}) = \int_\Omega |\varepsilon'(\vec{u})| dV \quad , \quad (5)$$

whereas $\vec{u}$ fulfils incompressibility, $\nabla \cdot \vec{u} = 0$, and satisfies all boundary conditions along Γ. The corresponding Euler equation turns out to be the Laplace equation,

$$\nabla^2 w = 0 \quad , \quad (6)$$

so $w(x, y)$ is a harmonic function within Ω.

1.2.1   Thin plate kinematics in consideration of large deflection (stress stiffening)

Kinematical assumptions within the framework of thin plate approximation are reflected in the displacement field,

$$\vec{u}(x, y, z) = \begin{pmatrix} \hat{u} \\ \hat{v} \\ \hat{w} \end{pmatrix} = \begin{pmatrix} u(x, y) \\ v(x, y) \\ w(x, y) \end{pmatrix} - z \begin{pmatrix} \phi_x \\ \phi_y \\ 0 \end{pmatrix} , \quad (7)$$

with

$$\frac{\partial w}{\partial x} = \phi_x, \quad \frac{\partial w}{\partial y} = \phi_y .$$

$u(x, y)$, $v(x, y)$ and $w(x, y)$ are the displacements of the mid-plane of the plate. The Green-Lagrange strain tensor for thin plates is [10]

$$E = \begin{pmatrix} \frac{\partial u}{\partial x} + \frac{1}{2}\left(\frac{\partial w}{\partial x}\right)^2 & \frac{1}{2}\left(\frac{\partial u}{\partial y} + \frac{\partial v}{\partial x} + \frac{\partial w}{\partial x}\frac{\partial w}{\partial y}\right) & 0 \\ \frac{1}{2}\left(\frac{\partial u}{\partial y} + \frac{\partial v}{\partial x} + \frac{\partial w}{\partial x}\frac{\partial w}{\partial y}\right) & \frac{\partial v}{\partial y} + \frac{1}{2}\left(\frac{\partial w}{\partial y}\right)^2 & 0 \\ 0 & 0 & -\frac{\partial u}{\partial x} - \frac{\partial v}{\partial y} - \frac{1}{2}\left(\left(\frac{\partial w}{\partial x}\right)^2 + \left(\frac{\partial w}{\partial y}\right)^2\right) \end{pmatrix} -$$
$$- z \begin{pmatrix} \frac{\partial^2 w}{\partial x^2} & \frac{\partial^2 w}{\partial x \partial y} & 0 \\ \frac{\partial^2 w}{\partial x \partial y} & \frac{\partial^2 w}{\partial y^2} & 0 \\ 0 & 0 & 0 \end{pmatrix} \quad (8)$$

whereas the strain component causing sheet thinning is determined from volume constancy. The second term of (8), representing the curvature of the plate mid-surface, causes no thinning and no volume change. This can be verified by the fact, that the trace vanishes if $w(x, y)$ is a harmonic function.

For further proceeding the area Ω can be divided into two parts with qualitatively different predominating deformation types.

1.2.2   Plastic bending, plastic hinge

The rigid circumference of the spotweld nugget acts like a plastic hinge, so the second term in (8), the curvature, is dominant, and the corresponding plastic work becomes (for the case of no work-hardening)

$$W_p^1 \approx \frac{Yt^2}{2\sqrt{3}} \oint_{\Gamma_1} \left| \frac{\partial w}{\partial n} \right| ds \quad, \tag{9}$$

where $\partial / \partial n$ means outward normal derivation along the inner circle.

1.2.3   Plastic stretching

In the course of out-of-plane deformation the first term in (8), representing the plastic membrane-type deformation, becomes more and more crucial. Additional neglect of in-plane displacements yield the following expression for plastic work (for the case of no work-hardening)

$$W_p^2 = \frac{Yt}{\sqrt{3}} \oint_{\Gamma} \frac{\partial w}{\partial n} w ds \quad. \tag{10}$$

The linearity of the governing differential equation (6) offers the development of a finite spotweld element by Trefftz formulation. It covers Hencky plasticity for the case of monotonic loading. Isotropic hardening can be accounted for by a piecewise perfectly-plastic cascaded flow curve.

1.3   Combination of the Linear Elastic and Rigid/Perfectly Plastic Model – Rheological approach

Both material models, the linear elastic and the rigid/perfectly plastic one, yield a stiffness matrix of the Trefftz element, K_e and K_p, respectively. Now, an elasto-plastic model can be deduced by the combination of these two sub-models by means of a rheological approach in the following way: The sub-models are connected in series, motivated by the assumptions that the addition of the elastic and plastic parts of the displacement gives the total displacement, whereas the level of reaction forces for both models are equal. The total stiffness matrix K by virtue of the serial connection is give by

$$K = \left(K_e^{-1} + K_p^{-1} \right)^{-1} \quad. \tag{11}$$

Of course, the rigid body modes of the stiffness matrices have to be omitted in order to achieve invertibility.

2   Failure (Instability) Criteria

Real tests show, that spotwelds under monotonic (non-oscillating) loads fail predominantly at the circumference of the nugget (within the base material) (see Fig.3). Instability due to the onset of local necking in this area proves to be the most important process limiting the ultimate force, which the spotweld can resist before failure occurs. This effect of instability can be implemented in the Trefftz spotweld model in a very natural way.
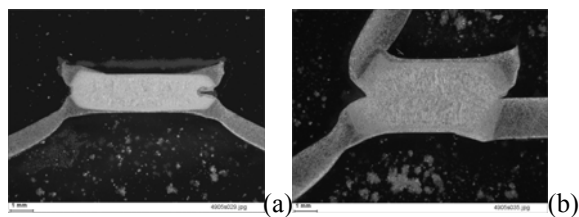

(a)   (b)

Fig. 3 Micrographs of failed spotwelds: (a) normal tension (90°-direction); (b) loaded under 30°-direction. The reason for failure is the onset of local necking of the base material in the vicinity of the nugget.

2.1 Spotweld-Weakening Due to Diffuse Necking along the Nugget-Circumference

The high resolution of the Trefftz strain field along the circumference of the spotweld nugget provides the opportunity to calculate the local thinning of the adjacent metal sheet every time step. The ratio of initial to the current thickness t/t_0 within the Trefftz-Element area Ω, and especially along its inner boundary, is given by the *zz*-component of the Green-Lagrange strain tensor (8)

$$\frac{t}{t_0} = 1 + E_{zz} = 1 - \frac{\partial u}{\partial x} - \frac{\partial v}{\partial y} - \frac{1}{2} \left(\left(\frac{\partial w}{\partial x} \right)^2 + \left(\frac{\partial w}{\partial y} \right)^2 \right), \tag{12}$$

and averaging of the ratio t/t_0 over the nugget circumference

$$\eta = \frac{1}{2\pi R} \oint_{\Gamma_1} \frac{t}{t_0} d\Gamma \,, \tag{13}$$

with spotweld radius R, yield a quantity η, which is a measure of the current spotweld-weakening. Now, this factor η is used to scale the block-matrices of the spotweld stiffness matrix (11) representing the coupling of degrees of freedom of the spotweld nugget only, K_{22}, and the mixed sub-matrix, which couples the nugget- with the polygon-nodes, K_{12},

$$K = \begin{pmatrix} K_{11} & K_{12} \\ K_{12}^T & K_{22} \end{pmatrix} \rightarrow K = \begin{pmatrix} K_{11} & \eta K_{12} \\ \eta K_{12}^T & \eta K_{22} \end{pmatrix}. \tag{14}$$

In this way the effect of softening due to diffuse necking is included, and it shows a good predictability for instability due to the onset of local necking (see Figs.4d,7).

3   User Element in ANSYS

The elasto-perfectly plastic spotweld element based on Trefftz formulation is implemented in ANSYS as User Element (UPF, User Programmable Feature). It has the capability of membrane-type and bending-type deformation by forming a plastic hinge at the circumference of the approximately rigid spotweld nugget. Additionally, the geometrical non-linearity due to the occurrence of in-plane stretching as a result of out-of plane displacement (stress stiffening) is taken into account. In most test-cases it converges satisfactory. There are altogether 5 user elements with 4 up to 8 polygon nodes, each with one mid-node (Fig.1c). Two mid-nodes can be coupled via constraints or by a beam element.

3.1   Example of Use

To prove the applicability of the Trefftz spotweld element in industrial applications a practical example of use is considered. It consists of a spot welded device with three clamps. Each clamp is pulled out monotonically (see Fig.4). The obtained force vs. displacement curves (Fig.4d) exhibit the realistic behaviour, a cascaded shape due to the successive failure of spotwelds.
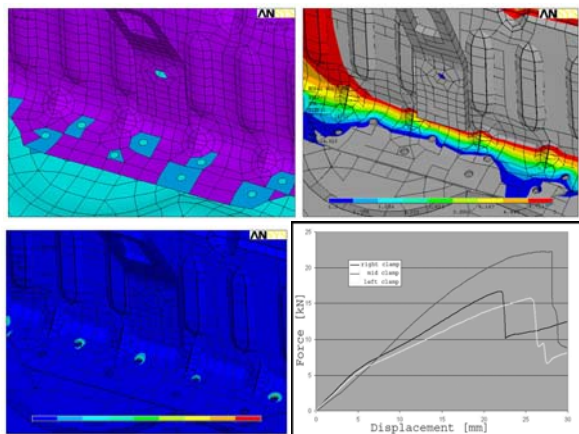

Fig. 4 Example of use for the Trefftz spotweld elements (a, upper left). The clamp, fixed at a spot welded device, is pulled out monotonically till the spotwelds start to fail successively; Contour plot of the transverse displacement (b, upper right); Contour plot of the equivalent plastic strain (c, lower left). The critical spotwelds are clearly observable; (d, lower right) shows the force vs. displacement curves for an arrangement of three clamps obtained from the simulation. The cascaded shape of the curves is due to the successive failure (instability) of spotwelds.

4   Implementation in Explicit FE-Codes

To make the benefit from Trefftz formulation applicable for explicit FE-codes an analogous model, made of beam elements, is constructed. The elasto-plastic beam parameters are calculated automatically in such a way, that the entire structure behaves similar to the corresponding elastic-plastic Trefftz element (Fig.5). This approach has essential advantages compared to standard methods. It provides realistic kinematical behaviour of the spotweld under crash loads, for example realistic twisting of the nugget due to shear loading, because it takes its circular shape and size into account. Numerical stability within the framework of explicit time integration is guaranteed by adapting the beam stiffness slightly if necessary.
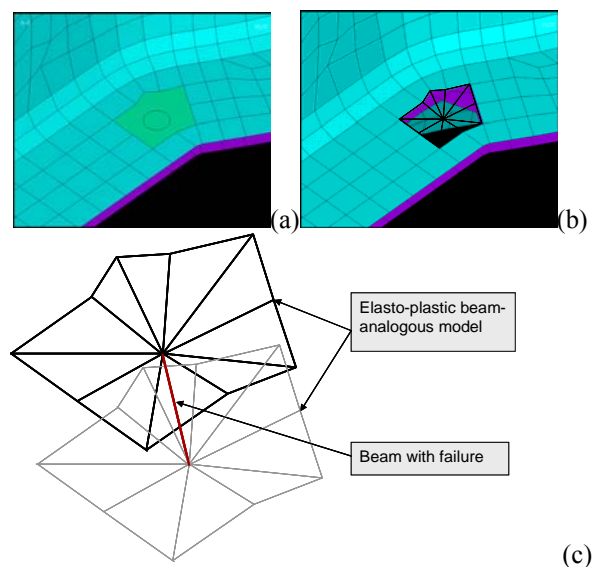

Fig. 5 The elasto-plastic spotweld element (hybrid Trefftz) (a) is replaced by a system of beam elements, that exhibits similar resultant behaviour. The analogous models made of beam elements are connected by a beam element including failure (b,c).

5   Validation

The validation of the Trefftz spotweld model is tested by means of the FAT KS tensile test configuration. It consists of a single-spot welded pair of metal bowls (see Fig.6a). They are clamped via flanges and pulled apart under distinct direction until full separation is reached. The force vs. displacement curves are measured and compared with the curves obtained from the finite element model (Fig.6b) including the Trefftz spotweld (see Fig.7).
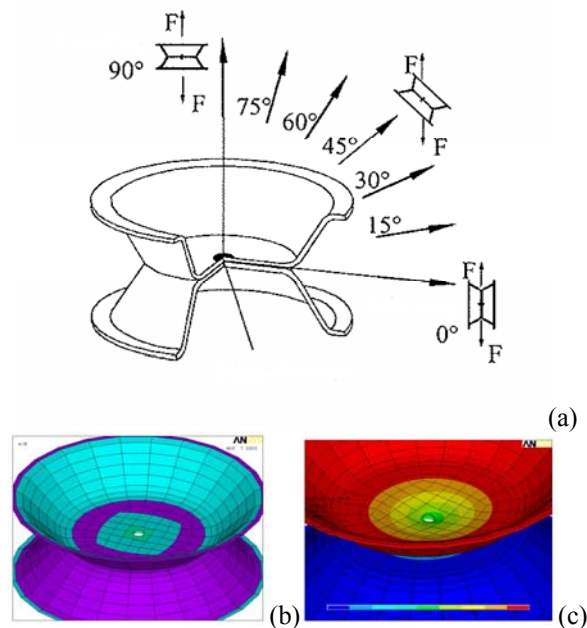
(a)

(b)   (c)

Fig. 6 The FAT KS tensile test configuration (a) is used to test the validity of the Trefftz spotweld model (b). The two single-spot welded metal bowls are pulled apart under distinct directions measuring the force vs. displacement curves; (c) Contour plot of the transverse displacement for the 30°-direction.
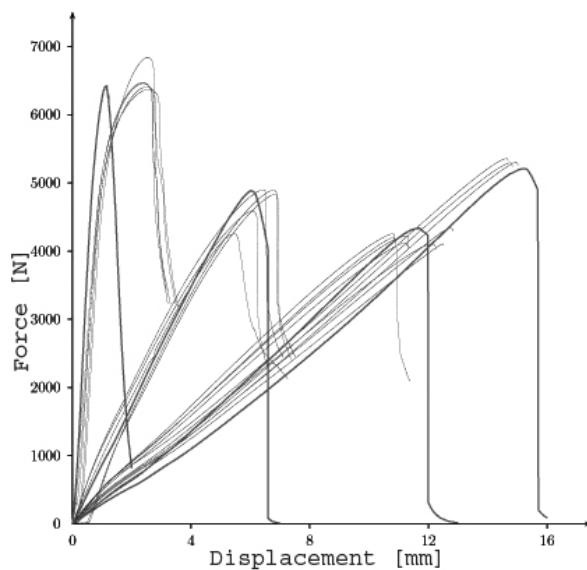

Fig. 7 Force vs. displacement curves for the 0°-,.30°-, 60°- and 90°-directions of the FAT KS tensile test (from right to the left). The darker curves are obtained from real tests, and the lighter ones are received from the finite element simulation with the Trefftz spotweld element.

The deviation of real shear test and simulation is probably due to the too stiff modeling of the clamping device. Comparison of the standard spotweld model of Ansys (multi point constraints, swgen) and the Trefftz spotweld model with equal mesh coarseness shows nearly equal expenditure of CPU calculation times (see Fig.8). The outstanding benefit of the Trefftz

formulation is that the failure predictability is independent of mesh coarseness, whereas the standard formulation requires expensive local mesh refinement.
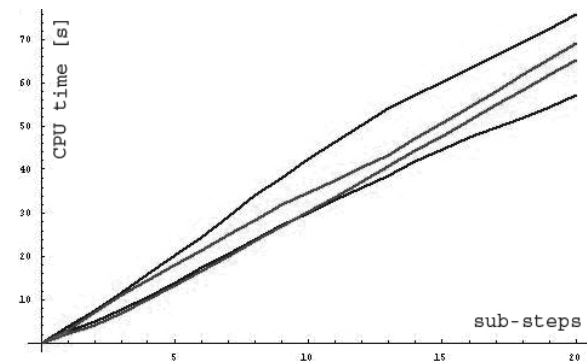

Fig. 8 CPU time vs. number of sub-steps for the FAT KS tensile test simulations. Darker curves: Trefftz spotweld; Lighter curves: Ansys standard spotweld (swgen).

6   Conclusion

A finite spotweld element based on hybrid Trefftz formulation is developed, with a rigid cylinder, representing the comparatively rigid nugget, and the surrounding area of the metal sheet, which is linked to the adjacent shell element structure via an arbitrary polygon. It covers elasto-plastic membrane- and bending- type deformations within the framework of Kirchhoff's thin-plate approximation. Hencky's deformation theory for a rigid-perfectly plastic material yield linear governing differential equations for the displacement field, by taking geometrical non-linearity (stress stiffening) into account. Plastic bending, which is concentrated at the rigid circumference of the spotweld nugget, is incorporated into the model by means of a circular plastic hinge. By definition the Trefftz-type solution satisfies a priori all governing differential equations within the element area and fulfils inner boundary conditions, leading to a high resolution of the stress/strain field in the vicinity of the spotweld nugget, and enables the introduction of more accurate stress/strain-based failure criteria. This elasto-plastic spotweld element is implemented both in implicit (ANSYS) and explicit (LS-Dyna, PAM-CRASH) finite-element codes. It provides good predictability of spotweld failure due to the onset of local necking (instability) at the circumference of the nugget without drawback concerning calculation time and convergence performance.

7   References

[1] A. H. ENGLAND. *Complex Variable Methods in Elasticity*, Wiley-Interscience, New York, 1971.

[2] TH. HEUBRANDTNER and T. AKGÜN. *Mathematical Modelling of Weld Phenomena 7*, Verlag der Technischen Universität Graz, 2005.

[3] R. HILL. The Mathematical Theory of Plasticity, Oxford, 1950.

[4] G. V. KOLOSOV. On an Application of Complex Function Theory to a Plane Problem of the Mathematical Theory of Elasticity, Yuriev, 1909.

[5] N. I. MUSKHELISHVILI. Some Basic Problems of the Mathematical Theory of Elasticity, Groningen, Noordhoof, 1953.

[6] G. ANZELLOTTI and M. GIAQUINTA. On the Existence of the Fields of Stresses and Displacements for an Elasto-Perfectly Plastic Body in Static Equilibrium, J. Math. pures et appl., 61, 1982, p. 219-244.

[7] R. PILTNER. *Special Finite Elements with Holes and Internal Cracks*, Int. J. for Num. Methods in Engineering 1985, 21,1471–1485.

[8] R. PILTNER. Recent Developments in the Trefftz Method for Finite Element and Boundary Element Applications, Advances in Engineering Software 1995, 24, 107–115.

[9] E. TREFFTZ. *Ein Gegenstück zum Ritz'schen Verfahren*, Proc. 2nd Int. Cong. on Applied Mechanics, Zürich 1929, 131–137.

[10] O. C. ZIENKIEWICZ and R. L. TAYLER. *The Finite Element Method - Solid Mechanics*, 2nd edn., Oxford, 2000.

[11] TH. HEUBRANDTNER, D. SCHERJAU and C. LIND. *Advanced Spotweld Failure Modelling Based on Trefftz Formulation*, 5th International Conference on Computation of Shell and Spatial Structures (IASS IACM 2005) Salzburg, 2005.